Analysis of Pressure Fluctuations in Fluidized Beds

David Falkowski and Robert C. Brown*

Center for Sustainable Environmental Technologies, Iowa State University, 286 Metals Development Building, Ames, Iowa 50011

Pressure fluctuations were measured in a fluidized bed and evaluated in the frequency domain. The objective of this research was to determine the effect of bed parameters on the power spectra from the corresponding pressure fluctuations. The motivation for this work is to develop pressure fluctuations as a diagnostic tool for fluidized-bed reactors and combustors. Pressure fluctuation data for a range of bed heights, fluidization velocities, particle sizes, particle densities, and bed temperatures were taken to determine the effect of these parameters on the power spectrum. The dominant frequency was a function of the height of the fluidized bed. Secondary peaks were not influenced by the height of the bed, although they did depend on the position of the probe in the bed. Peaks in power spectra were observed to shift in frequency as the gas superficial velocity through the bed was changed. Powders of different classification had distinctive power spectra. Group A powders behaved like first-order linear systems; group B powders showed similarities to second-order linear systems; and group D powders exhibited harmonic behavior in their power spectra. When pressure fluctuations were measured over a temperature range from ambient to above 500 °C, power spectra varied little when the ratio of the superficial velocity to the minimum fluidization velocity was held relatively constant.

1. Introduction

Fluidized beds have been utilized in industry for many years in such processes as coal gasification and catalytic cracking of hydrocarbons. From their initial use, researchers have recognized the link between a fluidized bed's performance and its pressure fluctuations. Even though a large number of studies have investigated this relationship, the phenomenon is still not well understood. The goal of this research is to increase the understanding of the pressure fluctuations in a fluidized bed. This will benefit several different areas of work associated with fluidized beds, including issues related to hydrodynamic and heat-transfer similitude,[1,2] chemical processes occurring in fluidized beds,[3,4] and the use of pressure fluctuations as a diagnostic tool for the fluidized bed's performance and fluidization regime identification.[5−8]

The testing and analysis methods used to evaluate fluidized-bed pressure fluctuations have varied widely among researchers. Brue and Brown investigated sampling and analysis techniques traditionally used to measure and interpret pressure fluctuations.[9−11] They were the first researchers to use Bode plots to study spectra obtained from pressure fluctuations. They noted that several spectral features such as multiple-peak phenomena were more easily recognized with Bode plots. The present study extends this previous work by using Bode plots to examine pressure data acquired over a range of bed heights, fluidization velocities, particle diameters, particle densities, and bed temperatures.

2. Background

2.1. Pressure Fluctuation Analysis Techniques. Both time- and frequency-domain analysis techniques have been used to describe pressure fluctuations in a fluidized bed. In the earliest studies of pressure fluctuations in fluidized beds, Tamarin[12] and Hiby[13] used visual observation of the pressure signals with time to determine the frequency of the pressure fluctuations. Kang et al.[14] were among the first to use signal analysis techniques to describe the time and frequency characteristics of the pressure fluctuations. These techniques included probability density functions, the root mean square of the pressure fluctuations, and the power spectral density.

Lirag and Littman[15] extended the analysis techniques used by Kang et al.[14] to include autocorrelation and cross-correlation functions. The autocorrelation function was used to determine if a periodic phenomenon existed in the pressure fluctuations, while the cross-correlation function was used to determine if the pressure fluctuations in the bed occurred slightly before the pressure fluctuations in the plenum. They used the time lag from the cross-correlation function and the distance between probes to calculate the propagation velocity of the pressure wave. Fan et al.[16] used these two functions in a similar manner. Clark et al.[17] also discussed the autocorrelation function, power spectral density, and fast Fourier transform techniques and provided examples of each with a slugging fluidized bed.

Brue[10] was the first researcher to use Bode plots to study the power spectra of fluidized beds. The Bode plot technique consists of the logarithm of the power spectrum plotted against the logarithm of the frequency. By performing this transformation, Brue discovered several important characteristics of the pressure fluctuations in the power spectrum that were not previously observed. First, low-magnitude, secondary peaks that were not apparent in power spectral density plots were easily observed in the Bode plots. Second, bubbling fluidized beds were shown to have characteristics (e.g., −40 dB/decade decay slopes) expected of second-order linear dynamical systems.

2.2. Pressure Fluctuation Characteristics in the Frequency Domain. The following section describes the relationship between fluidized-bed pressure fluctuations and the variables of bed height, fluidization

10.1021/ie030684u CCC: $27.50
Published on Web 06/10/2004

velocity, particle density/diameter, and bed temperature. Multiple-peak phenomena are included in the last section because they are observed in several of the power spectra.

2.2.1. Bed Height Effects. Hiby[13] was the first researcher to relate the periodic nature of pressure fluctuations in a fluidized bed to a "natural frequency" occurring in the bed. He developed an equation to predict this natural frequency:

$$\omega_n = \frac{2}{\pi}\sqrt{\frac{g(1-\epsilon)}{3H_{mf}\epsilon}} \quad (1)$$

In this equation, ω_n is the natural frequency of the bed, g is gravity, ϵ is the bed voidage, and H_{mf} is the bed height at minimum fluidization. Hiby estimated that eq 1 was valid for shallow beds with heights of about 10 particle diameters. As the bed height was increased, the fluctuations became more random. The relationship of frequency being inversely proportional to the square root of the bed height remained reasonably accurate for bed heights of up to 500 particle diameters. Other researchers have experimentally confirmed this relationship for bed depths extending to over 1000 particle diameters.[16,18,19] Sun et al.[20,21] developed a relationship in which the frequency was inversely proportional to the bed diameter, but subsequent work by Bi and Grace[22] showed that the appropriate independent variable was the bed height.

Verloop and Heertjes[23] concluded from their studies of fluidized beds that pressure fluctuations are due to bubble inception at low bed heights, which is consistent with the theory of Hiby,[13] but that slugging phenomena become dominant once a critical bed height is reached. This bed height is on the order of a few hundred particle diameters. Using an energy balance on the fluidized bed, they derived the following equation for the natural frequency of a "lower-height" bed:

$$\omega_n = \frac{1}{2\pi}\sqrt{\frac{g(2-\epsilon)}{H_{mf}\epsilon}} \quad (2)$$

This equation is valid up to a critical bed height, above which slugging occurs. This critical height, L_c, is given by the following equation:

$$L_c = \frac{400\pi\epsilon d_p u_{mf}}{(2-\epsilon)u} \quad (3)$$

In this equation, d_p is the particle diameter, u_{mf} is the superficial velocity at minimum fluidization, and u is the superficial velocity.

The frequency relationship for slugging (ω_s) is given by

$$\omega_s = 0.35\sqrt{\frac{gD_b}{H_{mf}}} \quad (4)$$

where D_b is the bed diameter. Baeyens and Geldart[24] also determined that the slugging frequency was a function of the bed diameter, and Roy et al.[25] developed a similar equation for the slugging frequency based on the bed height.

2.2.2. Fluidization Velocity Effects. The effect of the fluidization velocity on the power spectra of pressure fluctuations is not well understood. Researchers generally agree that the dominant frequency increases with increasing superficial velocity.[9,15,26] For example, Van der Schaaf et al.[26] found two peaks in the power spectra to increase with increasing superficial velocity before eventually becoming independent of the gas velocity. These authors did not provide a reason for this behavior, but many researchers ascribe it to bubble phenomena in fluidized beds. For example, Fan et al.[27] measured bubble rise velocities in several fluidization regimes, including bubbling, slugging, and turbulent fluidization. They showed that for the bubbling regime both the dominant frequency and the bubble rise velocity increased with increasing superficial velocity. At the transition between bubbling and slugging regimes, a "jumplike" drop in the bubble rise velocity was observed. This transition coincides with the transition from bubbling to slugging observed at the critical height presented by Verloop and Heertjes.[23]

2.2.3. Particle Diameter and Density Effects. Geldart[28] and Kunni and Levenspiel[29] have described the relationship between the particle diameter/density effects and fluidization regimes. As observed by these researchers, slugging (or turbulent churning) often occurs in beds fluidized with group D particles. The criteria for determining if a bed is slugging is generally concluded through visual observation,[24] but other methods involving the amplitude of the pressure fluctuations,[30] the occurrence of a minimum in the magnitude of pressure fluctuations,[24] or the ratio of the bubble size to the bed diameter[29] have been used. Power spectra from slugging beds generally have only a single peak or a peak that is of considerably greater magnitude than secondary peaks. Clark[17] provides an example of a power spectrum for a slugging bed of group D particles.

Often researchers do not distinguish between the results obtained from group A and B particles.[25,31] For example, Roy et al.[25] use frequency data from both group A and B particles to determine a correlation for the natural frequency of a slugging bed, while Dhodapkar and Klinzing[31] provide examples of power spectra from group A and B particles that appear similar.

2.2.4. Bed Temperature Effects. Very few studies have investigated the effect of temperature on pressure fluctuations in fluidized beds. Svoboda et al.[32] measured pressure fluctuations in a fluidized bed across a temperature range of 20−700 °C. For freely bubbling beds, their experiments showed that the dominant frequency increased significantly as the bed temperature increased for the ratio of superficial velocity to minimum fluidization velocity, U/U_{mf}, ranging between 1 and 1.3. This result agrees with several other researchers who used optical or capacitive probes to measure the bubble frequency over the same temperature range.[33−35] However, Fan et al.[36] observed a more complex dependence between the dominant frequency and temperature than that reported by Svoboda et al.[32]

2.2.5. Multiple-Peak Phenomena. In most of the studies discussed above, only the dominant frequency in the power spectra was reported. Svoboda et al.[32] were one of the few groups to describe multiple-peak phenomena arising from pressure data. They found three peaks in the power spectra that changed in frequency as the velocity was changed.

Kage et al.[37] studied pressure fluctuations in the plenum of a bubbling fluidized bed. In several cases, they observed three peaks in the power spectra, which they believed arose from the eruption of bubbles from

Table 1. Description of Instruments Used in Experimental Apparatus

device	model	range	accuracy (%)
Omega pressure transducer	PX142-001D5V	0−6900 Pa	1.3
Omega pressure transducer	PX163-2.5BD5V	±622 Pa	1.3
Omega pressure transducer	PX163-005BD5V	±1244 Pa	1.3
Omega pressure transducer	PX164-005D5V	0−1244 Pa	1.3
Alicat flow controller sensor	MC-500SLPM-D/CM	0−500 LPM	1.5
Omega rotameter	FL4613	0−566 LPM	2.5
Key Instruments rotameter	FR4000A36BL	0−94 LPM	3.0

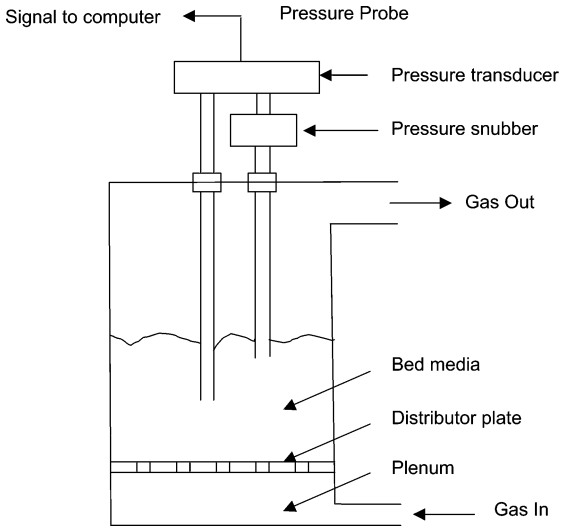

Figure 1. Arrangement of probe arms in a fluidized bed to measure the differential pressure (not to scale).

the bed, the generation of bubbles at the distributor plate, and the natural frequency of the fluidized media.

Svensson et al.[38] provided evidence of another multiple-frequency phenomenon: the disappearance of one peak and the emergence of another as the superficial velocity increased. Although this testing was done in a circulating fluidized bed and the increase in the superficial velocity needed to bring about this change was very large, it demonstrates that the emergence and disappearance of peaks is possible.

3. Experimental Apparatus and Procedure

3.1. Experimental Apparatus. The fluidized-bed reactor used in this work is part of a pyrolysis system located at the BECON Research Facility in Nevada, IA, and is described in detail in ref 39. The fluidized-bed reactor is constructed of stainless steel and had a diameter of 16.2 cm and a height of 100 cm. The distributor plate has 66 holes with diameter of 0.28 cm drilled in a square pattern, resulting in a 2% open area. A natural gas burner provided energy to the bed via a heating jacket annulus around the bed. House air was used as the fluidizing gas for testing.

The pressure probe used in this study consisted of a pair of stainless steel tubes, referred to as the probe arms, of 0.46 cm i.d. and 0.64 cm o.d. As shown in Figure 1, the probe arms were inserted vertically into the bed through an end plate at the top of the cylindrical fluidized-bed reactor and held in place with compression fittings (during testing at ambient temperature, a mounting bracket was substituted for the end plate to allow visual inspection of the fluidized bed). The horizontal (radial) distance between the two probe arms was 5.08 cm, and the vertical (axial) distance between the two arms was 2.54 cm. A wire mesh with 41% open area and a 65 μm open width covered the open ends of the probe arms to prevent bed particles from entering. The top end of the probe was attached to the pressure transducer through a short (less than 2 cm) section of plastic tubing.

Table 2. Bed Media with Corresponding Particle Mean Diameters and Densities

bed media	mean diameter (μm)	density (kg/m^3)
Badger 16 × 30 sand	878	2650
Badger 30 × 50 sand	494	2650
large glass beads	1125	2650
plastic spheres	200	630

The pressure transducers and flow measurement devices used in this testing are described in Table 1. The pressure transducer signal was recorded using National Instrument's hardware and software, and volumetric flow data were recorded by hand. Table 2 lists the bed media used in this testing, along with the mean particle diameter and the particle density. The tolerances on the large glass beads and plastic spheres were ±125 and ±50 μm, respectively.

3.2. Experimental Procedure. To begin the pressure acquisition procedure, the bed operating parameters were set to the given test conditions. About 123 000 data points were then acquired at a sampling frequency of 100 Hz. This sampling frequency allowed for the detection of all relevant frequencies. Because each spectrum's roll-off (the slope of the spectrum by which the signal is attenuated at higher frequencies[9]) was used to compare beds with different operating conditions, this sampling frequency also allowed for slope comparisons between the different conditions. The data analysis technique included the averaging of 29 power spectra and plotting of the power spectra on a Bode plot. This technique is discussed in ref 39 and has been used elsewhere.[9−11]

For the probe technique used in this study, both probe arms were submersed in the bed. One arm was connected directly to one of the two ports of the pressure transducer while the other arm was connected to the input side of a Ray Solid Body pressure snubber (model 023B). The output side of the pressure snubber was connected to the second port of the pressure transducer. The pressure snubber filtered out pressure fluctuations, providing a constant pressure signal to the pressure transducer. This allowed for more accurate pressure measurements through the use of a narrower-range pressure transducer that more fully encompassed the pressure fluctuations instead of a wider-range transducer that accounted for the higher average pressure and the pressure fluctuations. Several tests were performed that showed that the pressure signal through the pressure snubber was constant. To determine the minimum superficial velocity, a technique described by Fan et al.[40] was used. This technique involved slowly increasing the gas flow to the bed until small pressure fluctuations were seen in the pressure signal. This is the point of minimum fluidization, and the presence of

Experimental Operating Conditions for Figure 2

Bed media:	Badger 30x50 Sand	Bed height:	Given in figure (± 0.3 cm)
Mean particle diameter:	494 micron	Bed mass:	2638.71 ± 0.01 gm
			5277.41 ± 0.01 gm
			7916.11 ± 0.01 gm
			15832.23 ± 0.01 gm
Volumetric flow:	345 ± 7.5 LPM	Pressure probe position:	3.8 ± 0.2 cm
U/U_{mf}:	1.4	Particle density:	2600 ± 100 kg/m^3

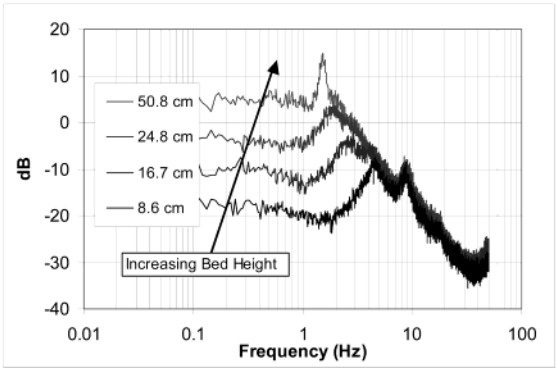

Figure 2. Power spectra at four different bed heights with the probe arm at a constant position from the distributor plate.

pressure fluctuations at this point was very apparent as compared to the constant pressure in a packed bed.

Because the bed height was somewhat difficult to measure accurately when the bed was fluidized, the mass of the bed media (e.g., sand) was measured with a Setra model 1000 scale. The media was weighed in increments of up to approximately 1000 g and added to the bed until the desired bed mass was attained. This was done so that nearly identical bed conditions (e.g., bed heights) could be achieved between tests that were not performed consecutively on the same day.

4. Results and Discussion

The following section describes the effect of several fluidized-bed parameters on the power spectra. These parameters include the bed height, superficial velocity, particle density, particle diameter, and bed temperature.

4.1. Influence of the Bed Height. To understand the influence of the bed height on the power spectrum, tests were performed at different bed heights with the probe arms positioned at a fixed distance above the distributor plate. Figure 2 shows power spectra for four different bed heights ranging from 8.6 to 50.8 cm with the probe arms 3.8 cm above the distributor plate.

Figure 2 shows that the dominant frequency decreases as the bed height increases. The shifting of the dominant peak with the bed height is well documented by other researchers.[13,23] For the four peaks of greatest magnitude, it was found that their frequencies were related to the bed height by the following power law:

$$f \propto h^{-0.63} \tag{5}$$

where f is the frequency of the peak, h is the fluidized-bed height, and the coefficient of determination (R^2) for this equation is 0.9604. This exponent (−0.63) is between values found in the literature for beds of less than 1 cm in height (−0.5)[13] and beds of greater than 1 m in height (−1.0).[25]

The Bode plot is characterized by a low-frequency horizontal asymptote (some cases are more clearly discerned than others) and a high-frequency roll-off of

Experimental Operating Conditions for Figure 3

Bed media:	Badger 30x50 Sand	Bed height:	Given in figure (± 0.3 cm)
Mean particle diameter:	494 micron	Bed mass:	3000.00 ± 0.01 gm to
			5100.00 ± 0.01 gm in
			steps of 300.00 gm
Volumetric flow:	345 ± 7.5 LPM	Pressure probe position:	Bed ht − 2.5 ± 0.2 cm
U/U_{mf}:	1.4	Particle density:	2600 ± 100 kg/m^3

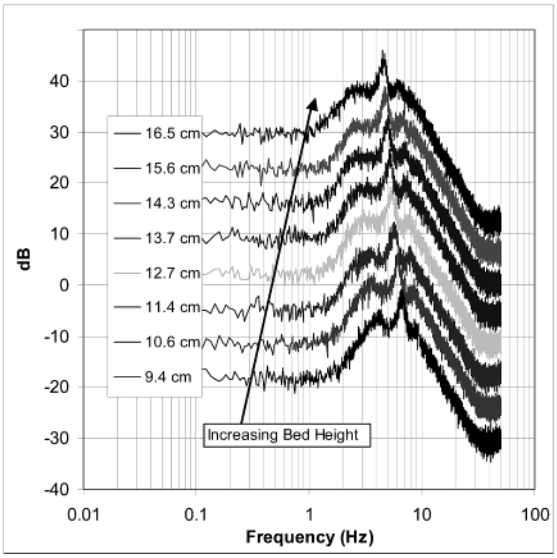

Figure 3. Power spectra at eight bed heights with the probe arm at a constant position of 2.5 cm below the bed surface for each test. The power spectra are offset by 6 dB to clarify any differences.

approximately constant slope. A secondary spectral peak at about 8 Hz frequently interrupts this roll-off. However, both before and after the 8 Hz peak, the slope of the Bode plot is approximately −40 dB/decade, which is characteristic of the Bode plots for second-order linear dynamical systems.[41] The secondary peak at 8 Hz is not a function of the bed height, which contrasts with the behavior of the dominant peaks documented here and in the literature. This secondary peak has not been reported previously in the literature. The probable reason for this oversight is the small magnitude of this and other secondary peaks, which are difficult to discern on conventional power spectral density plots.

Power spectra for different bed heights were also determined with the probe arm at a constant position with respect to the bed surface (as opposed to the previous tests that held the probes at a constant position with respect to the distributor plate). Figure 3 shows eight different bed heights in the range of 9.4−16.5 cm. For each of these tests, the probe arm was kept 2.5 cm below the surface of the bed.

The shifting of the dominant peak to lower frequencies with an increase in the bed height follows a power law given by

$$f \propto h^{-0.65} \tag{6}$$

with R^2 equal to 0.9984. This relationship is similar to eq 5 and agrees with the literature. When the arm position was kept near the surface as sand was added, the entire spectrum shifted to lower frequencies while the shape of the spectrum remained similar. This is in contrast with the power spectra of Figure 2, where the amplitude of the power spectrum remained constant above a frequency of 5 Hz for all probe arm positions.

4.2. Influence of the Superficial Velocity. To understand the effect of the superficial velocity on the

Experimental Operating Conditions for Figure 4

Bed media:	Badger 30x50 Sand	Bed height:	16.7 ± 0.3 cm
Mean particle diameter:	494 micron	Bed mass:	5277.41 ± 0.01 gm
Volumetric flow:	265 to 430 ± 7.5 LPM	Pressure probe position:	10.2 ± 0.2 cm
U/U_{mf}:	Given in parentheses	Particle density:	2600 ± 100 kg/m^3

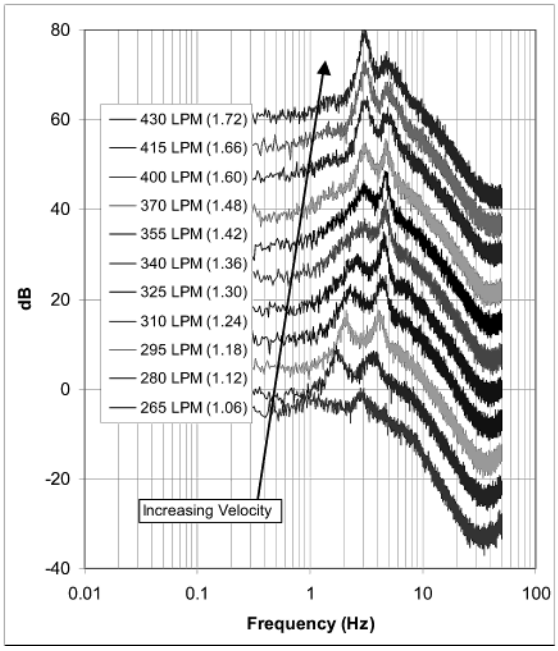

Figure 4. Power spectra from the bed operating at different U/U_{mf}. The power spectra are offset by 6 dB to clarify any differences. U/U_{mf} for each spectrum is listed in parentheses, with the corresponding volumetric flow in the legend.

power spectrum, tests were performed at different U/U_{mf}, which is the ratio of the superficial gas velocity in the bed to the superficial velocity at the minimum fluidization condition. In Figure 4, power spectra are shown for U/U_{mf} ranging from 1.06 (265 LPM) to a U/U_{mf} of 1.72 (430 LPM). The U/U_{mf} for each spectrum is listed in parentheses, with the corresponding volumetric flow rate in the legend.

When U/U_{mf} increased, peaks in the power spectra were found to shift in frequency and increase or decrease in magnitude relative to one another. The magnitude of each peak is shown to be a strong function of U/U_{mf}, increasing in magnitude with an increase in velocity. The two largest-magnitude peaks in the power spectrum at a U/U_{mf} of 1.06 occur at 1 and 3 Hz. When U/U_{mf} increases to 1.72, the two strongest peaks shift to 3 and 5 Hz. This trend of dominant frequencies increasing with velocity agrees with that of Van der Schaaf et al.[26]

The relative magnitude of the two strongest peaks also changes with increasing U/U_{mf}. For example, as U/U_{mf} increases from 1.24 to 1.60, the secondary peak at 2.1 Hz becomes the primary peak. Svoboda et al.[32] have observed this phenomenon and described it as a "jumplike change", but the Bode plot offers a more informative view of this phenomenon. Instead of peaks appearing and disappearing, the present data suggest that there is a gradual shift in dominance between the two peaks as the superficial velocity increases. This shifting in peak dominance may be attributed to a change in the fluidization regime. Regime changes have been observed in the frequency domain elsewhere, such as the work by Fan et al.,[27] which documented a shift in the dominant frequency in going from a bubbling to a slugging regime. A similar change in the fluidization regime may be occurring here.

Experimental Operating Conditions for Figure 5

Bed media:	Badger 30x50 Sand	Bed height:	8.3 ± 0.3 cm
Mean particle diameter:	494 micron	Bed mass:	2638.71 ± 0.01 gm
Volumetric flow:	295 to 415 ± 7.5 LPM	Pressure probe position:	2.5 ± 0.2 cm
U/U_{mf}:	Given in parentheses	Particle density:	2600 ± 100 kg/m^3

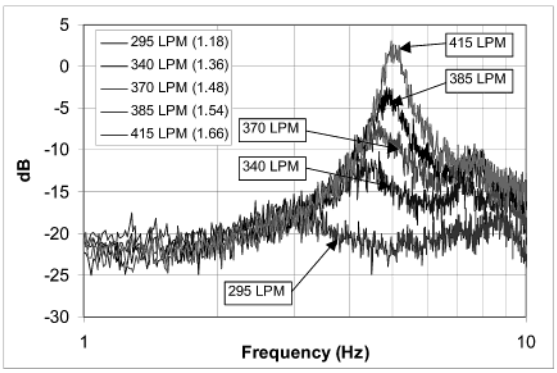

Figure 5. Power spectra showing the continuous growth of the dominant peak at five different superficial U/U_{mf}. The U/U_{mf} for each spectrum is listed in parentheses, with the corresponding volumetric flow in the legend.

Experimental Operating Conditions for Figure 6

Bed media:	Badger 16x30 Sand	Bed height:	34.0 ± 0.3 cm
Mean particle diameter:	878 micron	Bed mass:	10554.82 ± 0.01 gm
Volumetric flow:	479 ± 14.2 LPM	Pressure probe position:	10.2 ± 0.2 cm
U/U_{mf}:	1.3	Particle density:	2600 ± 100 kg/m^3

Bed media:	Glass beads	Bed height:	35.2 ± 0.3 cm
Mean particle diameter:	1.1 mm	Bed mass:	10554.82 ± 0.01 gm
Volumetric flow:	552 ± 14.2 LPM	Pressure probe position:	10.2 ± 0.2 cm
U/U_{mf}:	1.1	Particle density:	2600 ± 100 kg/m^3

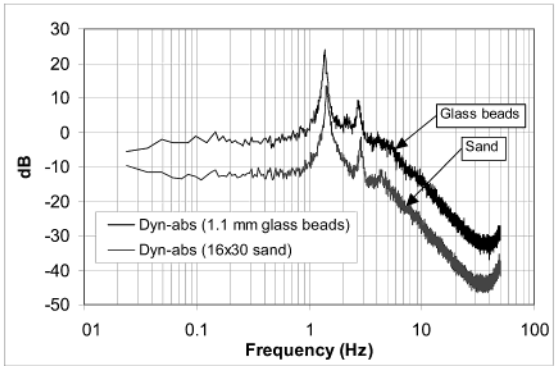

Figure 6. Presence of harmonics in the power spectra with group D glass beads and sand particles. The power spectra are offset by 10 dB to clarify any differences. In the accompanying table, operating conditions with two entries list the parameter associated with the Badger sand first and the glass beads second.

Figure 5 further illustrates the effect of U/U_{mf} on the power spectra, with U/U_{mf} varied from 1.18 to 1.66. The initially dominant peak at 3 Hz is gradually overtaken in magnitude by an initially smaller peak at 5 Hz as U/U_{mf} increases.

4.3. Influence of the Particle Diameter and Density. 4.3.1. Group D Particles. When beds with group D particles were fluidized, harmonics appeared in the power spectra. To further understand this phenomenon, pressure data were acquired for two different group D particles. Figure 6 compares the power spectra for 16 × 30 sand and 1.1 mm diameter glass beads.

Visual observation during these two tests revealed that slugging was occurring. As shown in this figure, the peak location and magnitude of the dominant and

Experimental Operating Conditions for Figure 7

Bed media:	Glass beads	Bed height:	35.2 ± 0.3 cm
Mean particle diameter:	1.1 mm	Bed mass:	10554.82 ± 0.01 gm
Volumetric flow:	552 ± 14.2 LPM	Pressure probe position:	22.9 ± 0.2 cm
U/U_{mf}:	1.1	Particle density:	2600 ± 100 kg/m^3

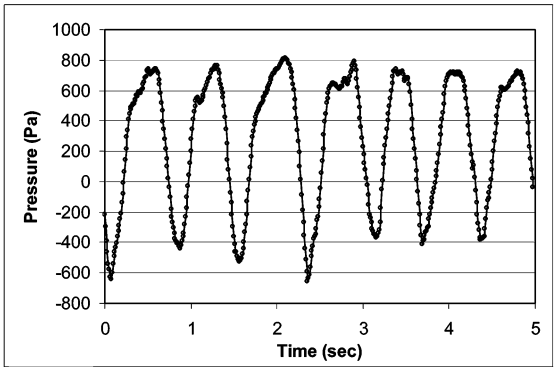

Figure 7. Presence of "square-wave" pressure fluctuations in the time domain with 1.1 mm glass beads.

Experimental Operating Conditions for Figure 8

Bed media:	Badger 16x30 Sand	Bed height:	34.0 ± 0.3 cm
Mean particle diameter:	878 micron	Bed mass:	10554.82 ± 0.01 gm
Volumetric flow:	479 ± 14.2 LPM	Pressure probe position:	22.9 ± 0.2 cm
U/U_{mf}:	1.3	Particle density:	2600 ± 100 kg/m^3

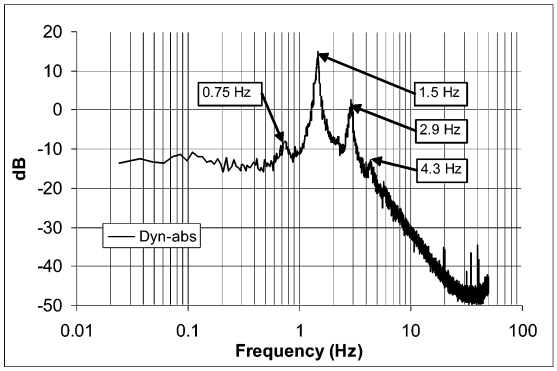

Figure 8. Presence of harmonics with Badger 16 × 30 sand.

secondary peaks (1.5 and 2.9 Hz, respectively) for the two spectra are very similar despite the difference in average particle diameters. Baeyens and Geldart[24] also note that the dominant frequency does not change for slugging beds at the same height with different particle diameters. The Bode plot makes the secondary peak discernible, whereas it would not be easily observable with the power spectral density technique.

To understand why harmonic frequencies were present, the pressure fluctuations from slugging beds were examined in the time domain. Figure 7 shows a 5 s pressure fluctuation signal for the 1.1 mm diameter glass beads. The pressure fluctuations resemble a square wave, and visual observation of the bed showed that the bed was slugging. Recalling that a square wave consists of multiples of the fundamental frequency, the appearance of harmonics for the slugging bed is not surprising.

The locations of the dominant and secondary peaks were examined to determine whether they were harmonics of a fundamental frequency. Figure 8 shows the power spectrum for a bed operating with Badger 16 × 30 sand. The locations of four peaks are labeled on this figure. Examining the peak frequencies in this figure shows that the peaks are close to whole multiples of each other. Taking the fundamental frequency to be 0.75 Hz, the other peaks at 1.5, 2.9, and 4.3 Hz are close to

Experimental Operating Conditions for Figure 9

Bed media:	Plastic spheres	Bed height:	29.8 ± 0.3 cm
Mean particle diameter:	200 micron	Bed mass:	2500.06 ± 0.01 gm
Volumetric flow:	37.8 ± 2.8 LPM	Pressure probe position:	22.9 ± 0.2 cm
U/U_{mf}:	2.0	Particle density:	630 ± 100 kg/m^3

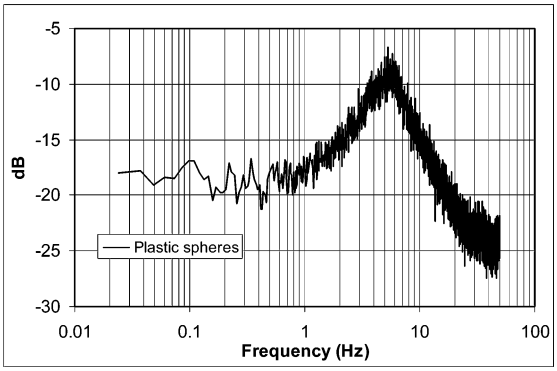

Figure 9. Power spectra with low-density plastic particles showing first-order behavior.

the second, fourth, and sixth harmonics. The dominant peak (1.5 Hz and 14 dB) and second largest peak in magnitude (2.9 Hz and 2 dB) are easily recognizable in Figure 8, but the magnitudes in the power spectrum are different by a factor of 15. This large difference in magnitude makes it difficult to discern the second peak when viewed with techniques such as the power spectral density.

Tests were also performed with steel beads to determine the effect of high-density particles on the power spectrum.[39] These tests showed that harmonics similar to those observed in Figure 8 were present in the power spectrum. With the steel particles, the square-wave phenomenon is associated with the larger gas forces needed to move the heavier particles. For example, a bubble in a steel-particle bed needs more force to displace the particles compared to a bubble in a sand-particle bed.

4.3.2. Group A Particles. Pressure data in a fluidized bed of group A particles were generated using plastic beads of 200 μm diameter and a specific density of 0.63. The Bode plot for these particles, illustrated in Figure 9, has a slope of −20 dB/decade, which corresponds to a first-order linear system. Why fluidized beds of group A particles should behave like first-order systems while beds of group B and D particles should behave like second-order linear systems is not readily understood. The simplest hydrodynamic example of a first-order system is a continuously stirred tank reactor.[41] The emulsion phase in a fluidized bed is often assumed to behave as a continuously stirred tank reactor;[42] thus, this result suggests that the flow of gas through this bed of group A particles was predominately through the emulsion phase. However, it is widely accepted that a proportionately larger amount of gas flows through the emulsion phase of beds of group B and D particles than occurs for group A particles.[42] Further investigations will be required to understand the origin of this first-order response in beds of small, low-density powders.

4.3.3. Summary of the Particle Diameter and Density Effects. The previous figures showed several differences in spectra that depended on the particle diameter and density. These included first-order characteristics (e.g., Figure 9), multiple-peak phenomena occurring in the bed (e.g., Figure 2), and harmonic

Particle data for Figure 10

Reference number	Particle type	Mean diameter	Density
1	Plastic	200 micron	630 kg/m^3
2	Sand	494 micron	2600 kg/m^3
3	Sand	878 micron	2600 kg/m^3
4	Glass	1100 micron	2600 kg/m^3
5	Steel	390 micron	7600 kg/m^3

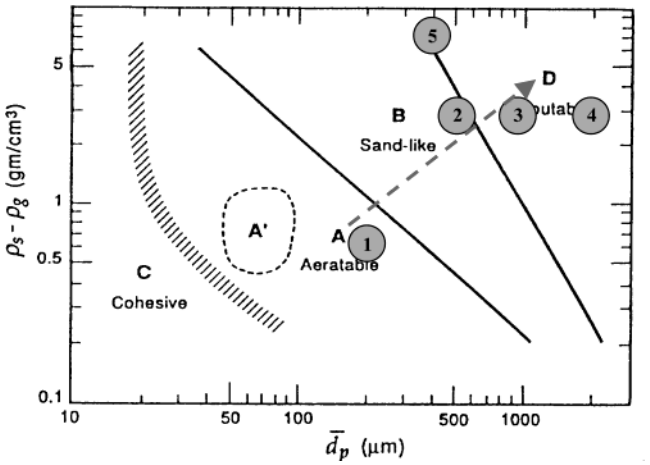

Figure 10. Geldart classification system with the plastic (1), sand (2 and 3), glass (4), and steel (5) particles examined in this research imposed on the figure.

behavior (e.g., Figure 8). To understand these characteristics better, the Geldart classification system was reexamined with the types of particles used in this research. Figure 10 shows the Geldart classification system,[14] with the five types of particles tested in this research noted on the figure. Particle information is listed in the accompanying table.

Following the dashed arrow in Figure 10, the bubble size generally increases from relatively small bubbles with the group A particles to larger bubbles with the group B particles to slugs with the group D particles. This transition through the Geldart groups is accompanied by first-order dynamics (group A), second-order dynamics with multiple-peak phenomena (group B), and harmonic behavior (group D), respectively. Because the change in the spectrum characteristics occurs at the transition between particle classifications, they are likely linked to the same bubble effect phenomena that account for the classification differences (e.g., square-wave pressure fluctuations from slugging yielding the harmonics).

4.4. Influence of the Temperature. The effect of the temperature on the power spectrum is not well understood. To study this effect, pressure fluctuation data were acquired with the bed temperatures ranging from 21 to 512 °C. The bed height and probe position were constant for all tests. Figure 11 shows the resulting power spectra for these tests, with U/U_{mf} listed in parentheses after the bed temperature in the legend. Both the superficial velocities and minimum fluidization velocities were evaluated at the bed temperature for the test. For these nine spectra, U/U_{mf} was in the range of 1.3−1.5.

In Figure 11, the dominant frequency (4−5 Hz) and two secondary frequencies (2−3 and 6−7 Hz) remain constant throughout the temperature range. The dominant frequency varied within a 1 Hz range (4−5 Hz),

Experimental Operating Conditions for Figure 11

Bed media:	Badger 30x50 Sand	Bed height:	16.8 ± 0.3 cm
Mean particle diameter:	494 micron	Bed mass:	5277.41 ± 0.01 gm
Volumetric flow:	345, 204, 192, 146, 118, 96, 98, 81, and 66 ± 7.5 LPM	Pressure probe position:	14.0 ± 0.2 cm
U/U_{mf}:	Given in parentheses	Particle density:	2600 ± 100 kg/m^3

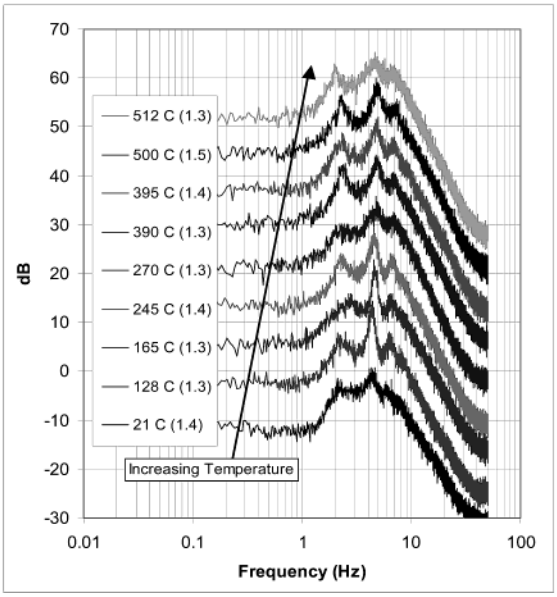

Figure 11. Power spectra at bed temperatures ranging from 21 to 512 °C with U/U_{mf} set between 1.3 and 1.5. The power spectra are offset by 8 dB to clarify any differences.

Experimental Operating Conditions for Figure 12

Bed media:	Badger 30x50 Sand	Bed height:	16.8 ± 0.3 cm
Mean particle diameter:	494 micron	Bed mass:	5277.41 ± 0.01 gm
Volumetric flow:	70.2, 81.0, 91.8, 102.6, 113.4, and 124.2 ± 7.5 LPM	Pressure probe position:	14.0 ± 0.2 cm
U/U_{mf}:	Given in legend	Particle density:	2600 ± 100 kg/m^3

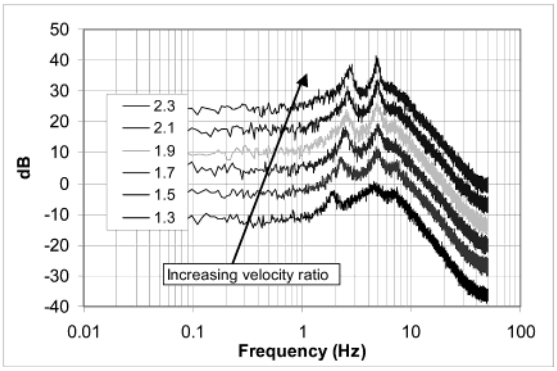

Figure 12. Power spectra at a bed temperature of 512 °C with U/U_{mf} varied from 1.3 to 2.3. The power spectra are offset by 6 dB to clarify any differences.

which agreed with the results of Fan et al.[36] Furthermore, the Bode plots show that the secondary peaks and general shape of the power spectra remain fairly constant for the given temperature range.

Superficial velocity tests were also performed with the same operating conditions as those in the previous figure at 512 °C, except that U/U_{mf} was varied from 1.3 to 2.3. The tests shown in Figure 12 were performed to understand the effect of the superficial velocity on the peaks in the power spectra.

The two largest peaks (1.9−2.9 and 4.6−5.0 Hz) showed a growth in magnitude with increasing velocity

similar to velocity tests at ambient temperature (Figure 4). The main difference between these two figures is that the dominant peak at the highest flow rate in Figure 4 was a secondary peak at lower flow rates, whereas the dominant peak remained at 4−5 Hz in all of the spectra shown in Figure 12. If changes in the superficial velocity produce changes in the secondary peaks of the power spectrum, these results may explain the wide scatter and odd trends in the data of Fan et al.[36] The testing shown in Figures 11 and 12 provides initial information for understanding the effect of the temperature on the multiple peaks in the power spectra.

5. Conclusions

Bode plots proved useful in studying the power spectra of pressure fluctuations obtained from fluidized beds and offer a new perspective on fluidized beds as dynamical systems. The work confirmed the results obtained by other researchers as well as highlighted phenomena not previously recognized. For example, Bode plot analysis revealed the dependence of the primary peak frequency on the bed height as well as discerned that the frequency of a previously unrecognized secondary peak was independent of the bed height. The Bode plot also helped to recognize that the difficulty in interpreting the effect of the superficial velocity on the spectral position of the primary peak was a result of two peaks existing in the spectra, which grew in magnitude relative to one another as the superficial velocity changed. Bode plots were used to investigate the role of Geldhart particle classification on pressure fluctuations. The Bode plots obtained by fluidizing group D particles contained harmonic frequencies, arising from the square-wave pattern of pressure in the time domain. The Bode plots for group A particles resembled those of first-order linear systems, which might reflect the predominance of gas flow through the emulsion phase of the fluidized media. Finally, Bode plot analysis was used to show that temperature had little effect on the spectral characteristics.

Acknowledgment

This work was supported in part by the Iowa Energy Center under Grant 98-05 and by the Center for Sustainable Environmental Technologies.

Nomenclature

d_p = particle diameter (μm)
f = natural frequency (Hz)
g = gravitational constant (m/s^2)
H_{mf} = bed height at minimum fluidization (m)
h = bed height (m)
L_c = critical bed height (m)
R = coefficient of determination
u = superficial velocity (cm/s)
u_{mf} = superficial velocity at minimum fluidization (cm/s)

Abbreviation

LPM = liters per minute

Greek Symbols

ω_n = natural frequency of the bed (rad/s)
ω_s = slugging frequency of the bed (rad/s)
ϵ = voidage

Literature Cited

(1) Nicastro, M. T.; Glicksman, L. R. Experimental verification of scaling relationships for fluidized beds. *Chem. Eng. Sci.* **1984**, *19* (9), 1381−1391.

(2) Glicksman, L. R.; Hyre, M. R.; Farrell, P. A. Dynamic similarity in fluidization. *Int. J. Multiphase Flow* **1994**, *20*, 331−386.

(3) Davidson, J. F. The two-phase theory of fluidization: successes and opportunities. *AIChE Symp. Ser.* **1991**, *87* (No. 281), 1−12.

(4) Zukowski, W. The pressure pulses generated by the combustion of natural gas in bubbling fluidized beds. *Combust. Flame* **2002**, *130*, 15−26.

(5) Schouten, J. C.; van den Bleek, C. M. Monitoring the quality of fluidization using the short-term predictability of pressure fluctuations. *AIChE J.* **1998**, *44* (1), 48−60.

(6) Trnka, O.; Vesely, V.; Hartman, M. Identification of the state of a fluidized bed by pressure fluctuations. *AIChE J.* **2000**, *46* (3), 509−514.

(7) Bai, D.; Shibuya, E.; Nakagawa, N.; Kato, K. Characterization of gas fluidization regimes using pressure fluctuations. *Powder Technol.* **1996**, *87*, 105−111.

(8) Fan, L. S.; Satija, S.; Wisecarver, K. Pressure fluctuation measurements and flow regime transitions in gas−liquid−solid fluidized beds. *AIChE J.* **1986**, *32* (2), 338−340.

(9) Brue, E. Pressure fluctuations as a diagnostic tool for fluidized beds. Ph.D. Dissertation, Iowa State University, Ames, IA, 1996.

(10) Brue, E. Process model identification of circulating fluidized bed hydrodynamics. M.S. Thesis, Iowa State University, Ames, IA, 1994.

(11) Brown, R. C.; Brue, E. Resolving dynamical features of fluidized beds from pressure fluctuations. *Powder Technol.* **2001**, *119*, 68−80.

(12) Tamarin, A. I. The origin of self-excited oscillations in fluidized beds. *Int. Chem. Eng.* **1964**, *4* (1), 50−54.

(13) Hiby, J. W. Periodic phenomena connected with gas−solid fluidization. *Proceedings of the International Symposium on Fluidization*, Eindhoven, The Netherlands, 1967; The Netherlands University Press: Amsterdam, The Netherlands, 1967; p 99.

(14) Kang, W. K.; Sutherland, J. P.; Osberg, G. L. Pressure fluctuations in a fluidized bed with and without screen cylindrical packings. *Ind. Eng. Chem. Fundam.* **1967**, *6* (4), 499−504.

(15) Lirag, R. C., Jr.; Littman, H. Statistical study of the pressure fluctuations in a fluidized bed. *AIChE J.* **1971**, *67* (116), 11−22.

(16) Fan, L. T.; Ho, T. C.; Hiraoka, S.; Walawender, W. P. Pressure fluctuations in a fluidized bed. *AIChE J.* **1981**, *27* (3), 388−396.

(17) Clark, N. N.; McKenzie, E. A., Jr.; Gautam, M. Differential pressure measurements in a slugging fluidized bed. *Powder Technol.* **1991**, *67*, 187−199.

(18) Baskakov, A. P.; Tuponogov, V. G.; Filippovsky, N. F. A study of pressure fluctuations in a bubbling fluidised bed. *Powder Technol.* **1986**, *45*, 113−117.

(19) Sadasivan, S.; Barreteau, D.; LaGuerie, C. Studies on frequency and magnitude of fluctuations of pressure drop in gas−solid fluidized beds. *Powder Technol.* **1980**, *26*, 67−74.

(20) Sun, J.; Chen, M. M.; Chao, B. T. On the fluctuation motions due to surface waves in gas fluidized beds. In *Proceedings of the First World Conference on Experimental Heat Transfer, Fluid Mechanics and Thermodynamics*, Dubrovnik, 1988; Shah, R. K., Ganic, E. N., Yang, K. T., Eds.; Elsevier: New York, 1988; p 1310.

(21) Sun, J.; Chen, M. M.; Chao, B. T. Modeling of solids global fluctuations in bubbling fluidized beds by standing surface waves. *Int. J. Multiphase Flow* **1994**, *20*, 315−338.

(22) Bi, H. T.; Grace, J. R. Comment on 'Modeling of solids global fluctuations in bubbling fluidized bed by standing waves' by Sun et al. *Int. J. Multiphase Flow* **1996**, *22* (1), 203−205.

(23) Verloop, J.; Heertjes, P. M. Periodic pressure fluctuations in fluidized beds. *Chem. Eng. Sci.* **1974**, *29*, 1035−1042.

(24) Baeyens, J.; Geldart, D. An investigation into slugging fluidised beds. *Chem. Eng. Sci.* **1974**, *29*, 255−265.

(25) Roy, R.; Davidson, J. F.; Tuponogov, V. G. The velocity of sound in fluidized beds. *Chem. Eng. Sci.* **1990**, *45* (11), 3233−3245.

(26) Van der Schaaf, J.; Schouten, J. C.; Johnsson, F.; van den Bleek, C. M. Multiples modes of bed mass oscillation in gas−solids fluidized beds. ASME: Proceedings of the 15th International Conference on Fluidized Bed Combustion, 1999; Paper FBC99-0201.

(27) Fan, L. T.; Ho, T. C.; Walawender, W. P. Measurements of the rise velocities of bubbles, slugs, and pressure waves in a gas−solid fluidized bed using pressure fluctuation signals. *AIChE J*. **1983**, *29* (1), 33−39.

(28) Geldart, D. Characterization of fluidized powders. In *Gas Fluidization Technology*; Geldart, D., Ed.; John Wiley & Sons: Chichester, U.K., 1980; pp 1−52.

(29) Kunni, D.; Levenspiel, O. *Fluidization Engineering*; Butterworth-Heinemann: Boston, 1991.

(30) Leva, M.; Weintaub, M.; Grumnmer, M.; Pollchik, M.; Storch, H. *U.S. Bur. Mines Bull.* **1951**, 504.

(31) Dhodapkar, S. V.; Klinzing, G. E. Pressure fluctuation analysis for a fluidized bed. In *Fluid-Particle Processes, AIChE Symposium Series*; Weimer, A. W., Ed.; AIChE: New York, 1993.

(32) Svoboda, K.; Cermak, J.; Hartman, M.; Drahos, J.; Selucky, K. Pressure fluctuations in gas-fluidized beds at elevated temperatures. *Ind. Eng. Chem. Process Des. Dev.* **1983**, *22*, 514−520.

(33) Otake, T.; Tone, S.; Kawashima, M.; Shibata, T. Behavior of rising bubbles in a gas-fluidized bed at elevated temperature. *J. Chem. Eng. Jpn.* **1975**, *8* (5), 388−392.

(34) Mii, T.; Yoshida, K.; Kunii, D. Temeprature-effects on the characteristics of fluidized beds. *J. Chem. Eng. Jpn.* **1973**, *6* (1), 100−102.

(35) Kai, T.; Furusaki, S. Behavior of fluidized beds of small particles at elevated temperatures. *J. Chem. Eng. Jpn.* **1985**, *18* (2), 113−118.

(36) Fan, L. T.; Huang, Y. W.; Neogi, D.; Yutani, N. Statistical analysis of temperature effects on pressure fluctuations in a gas−solid fluidized bed. *Fluidization '85* **1985**, 37−50.

(37) Kage, H.; Iwasaki, N.; Matsuno, Y. Frequency analysis of pressure fluctuations in plenum as a diagnostic method for fluidized beds. In *Fluid-Particle Processes, AIChE Symposium Series*; Weimer, A. W., Ed.; AIChE: New York, 1993.

(38) Svensson, A.; Johnsson, F.; Leckner, B. Fluidization regimes in non-slugging fluidized beds: the influence of pressure drop across the air distributor. *Powder Technol.* **1996**, *86*, 299−312.

(39) Falkowski, D. T. The analysis and modeling of pressure fluctuations in a fluidized-bed. Ph.D. Dissertation, Iowa State University, Ames, IA, 2003.

(40) Fan, L. T.; Huang, Y. W.; Yutani, N. Determination of the lower bound minimum fluidization velocity: application at elevated temperatures. *Chem. Eng. Sci.* **1986**, *41* (1), 189−192.

(41) Smith, C. A.; Corripio, A. B. *Principles and Practice of Automatic Process Control*; John Wiley & Sons: New York, 1985.

(42) Kunii, D.; Levenspiel, O. *AIChE Symp. Ser.* **1988**, *84* (No. 262).

Received for review August 22, 2003
Revised manuscript received May 3, 2004
Accepted May 3, 2004

IE030684U